Hydrogel–mesh composite for wound closure

Yang Gao[a], Xiuyuan Han[a], Jiaojiao Chen[a], Yudong Pan[a], Meng Yang[a], Linhe Lu[b], Jian Yang[b], Zhigang Suo[c,1], and Tongqing Lu[a,1]

[a]State Key Lab for Strength and Vibration of Mechanical Structures, Soft Machine Lab, School of Aerospace Engineering, Xi'an Jiaotong University, Xi'an 710049, China; [b]Department of Cardiovascular Surgery, Xijing Hospital, Air Force Medical University, Xi'an 710032, China; and [c]Kavli Institute for Bionano Science and Technology, School of Engineering and Applied Sciences, Harvard University, Cambridge, MA 02138

Contributed by Zhigang Suo, May 29, 2021 (sent for review February 20, 2021); reviewed by Metin Sitti and Shu Yang

During operations, surgical mesh is commonly fixed on tissues through fasteners such as sutures and staples. Attributes of surgical mesh include biocompatibility, flexibility, strength, and permeability, but sutures and staples may cause stress concentration and tissue damage. Here, we show that the functions of surgical mesh can be significantly broadened by developing a family of materials called hydrogel–mesh composites (HMCs). The HMCs retain all the attributes of surgical mesh and add one more: adhesion to tissues. We fabricate an HMC by soaking a surgical mesh with a precursor, and upon cure, the precursor forms a polymer network of a hydrogel, in macrotopological entanglement with the fibers of the surgical mesh. In a surgery, the HMC is pressed onto a tissue, and the polymers in the hydrogel form covalent bonds with the tissue. To demonstrate the concept, we use a poly(*N*-isopropylacrylamide) (PNIPAAm)/chitosan hydrogel and a polyethylene terephthalate (PET) surgical mesh. In the presence a bioconjugation agent, the chitosan and the tissue form covalent bonds, and the adhesion energy reaches above 100 J·m^{-2}. At body temperature, PNIPAAm becomes hydrophobic, so that the hydrogel does not swell and the adhesion is stable. Compared with sutured surgical mesh, the HMC distributes force over a large area. In vitro experiments are conducted to study the application of HMCs to wound closure, especially on tissues under high mechanical stress. The performance of HMCs on dynamic living tissues is further investigated in the surgery of a sheep.

surgical mesh | hydrogel | wet adhesion | wound closure

Surgical meshes are used extensively in surgery (1–7). A mesh is flexible in bending to conform to the curved surface of a tissue but is stiff in stretch to bear tension. The mesh is biocompatible and is permeable to water and other molecules. A mesh can be fastened to a tissue by sutures, staples, and spiral tacks, but these methods are time-consuming and may cause complications, such as nerve injury and chronic postoperation pain (8–10). A mesh can also be fastened to a tissue by glue (11–13). The glue cures in the pores of the mesh and forms bonds with the surface of the tissue. The glued mesh has been used as a sealant in hernia repair (6, 11), lung surgery (14, 15), bone marrow transplantation (16), spinal surgery (17, 18), and hepatic resection without biliary reconstruction (19, 20). A commonly used tissue glue, fibrin, is weak, so that the glued mesh is only applicable in surgeries when tissues bear low forces. For tissues under high mechanical stress, the glue is still unable to replace sutures, staples, and spiral tacks (21–25). To achieve wider applications, there is great demand to add one more attribute to surgical meshes: strong adhesion to tissues.

Here, we develop a class of surgical materials to achieve strong adhesion with tissues. We place a surgical mesh in a glass mold, pour a precursor of hydrogel into the mold, let the precursor soak into the interconnected pores between the fibers of the surgical mesh, and cure the precursor in situ into a hydrogel of a covalent polymer network. The structure of such a hydrogel–mesh composite (HMC) differs from that of an interpenetrating polymer network (IPN). The diameter of a fiber in the surgical mesh is ~20 μm (*SI Appendix*, Fig. S1), which is much larger than the length of a polymer chain. In the HMC, the hydrogel fills the pores, in topological entanglement with the surgical mesh at the scale of individual fibers. By contrast, in an IPN, two polymer networks are in topological entanglement at the scale of individual polymer chains. Once the HMC contacts a tissue, the surgical mesh and the tissue adhere through the hydrogel. To achieve strong adhesion, the hydrogel is designed to fulfill the following requirements. The hydrogel connects with the surgical mesh by forming a polymer network in topological entanglement with the fibers of the surgical mesh. The hydrogel and tissue have complementary functional groups for strong adhesion. The hydrogel has long polymer chains of two types: Type I polymers form a covalent network, and type II polymers carry functional groups for adhesion to a tissue (Fig. 1*A*). To peel the HMC from the tissue, the strong bonds between the type II polymers and the tissue transmit force into the covalent network of the type I polymers. Before a single bond between a type II polymer and the tissue breaks, the type II polymer distributes tension to nearby type I polymers through intermolecular interactions and physical entanglement. Breaking the single bond releases not only the chemical energy of the bond, but also much of the elastic energy stored in the nearby polymers. This stress deconcentration greatly amplifies adhesion toughness. In contact with a wet tissue for a long time, a hydrogel is prone to swell, which embrittles adhesion. In our design, the type I polymers have adjustable hydrophobicity. In contact with the tissue, the type I polymers become hydrophobic, so that the hydrogel is swell-resistant.

When the HMC is used to close a wound, the surgical mesh works as a skeleton to distribute force under tension (Fig. 1*B*).

Significance

Many surgeries require surgical mesh to be attached firmly at target areas to strengthen tissues, support organs, or repair wounds. Common methods of attachment include sutures, staples, and spiral tacks, but they damage tissues and prolong surgeries. Adhesion has been considered a promising alternative method to attach surgical meshes to tissues, but existing approaches of adhesion are too weak for most applications. Here, we develop composites of hydrogels and surgical meshes that can adhere to tissues firmly and stably. We demonstrate the applications of the hydrogel–mesh composites to wound closure, especially on tissues under high pressure or great tension.

Author contributions: Y.G., Z.S., and T.L. designed research; Y.G., X.H., J.C., and Y.P. performed research; Y.G., Z.S., and T.L. analyzed data; Y.G., Z.S., and T.L. wrote the paper; M.Y. contributed schematic plot; and L.L. and J.Y. contributed medical guidance.

Reviewers: M.S., Max-Planck-Institut fur Intelligente Systeme; and S.Y., University of Pennsylvania.

The authors declare no competing interest.

[1]To whom correspondence may be addressed. Email: suo@seas.harvard.edu or tongqinglu@mail.xjtu.edu.cn.

This article contains supporting information online at https://www.pnas.org/lookup/suppl/doi:10.1073/pnas.2103457118/-/DCSupplemental.

Published July 6, 2021.

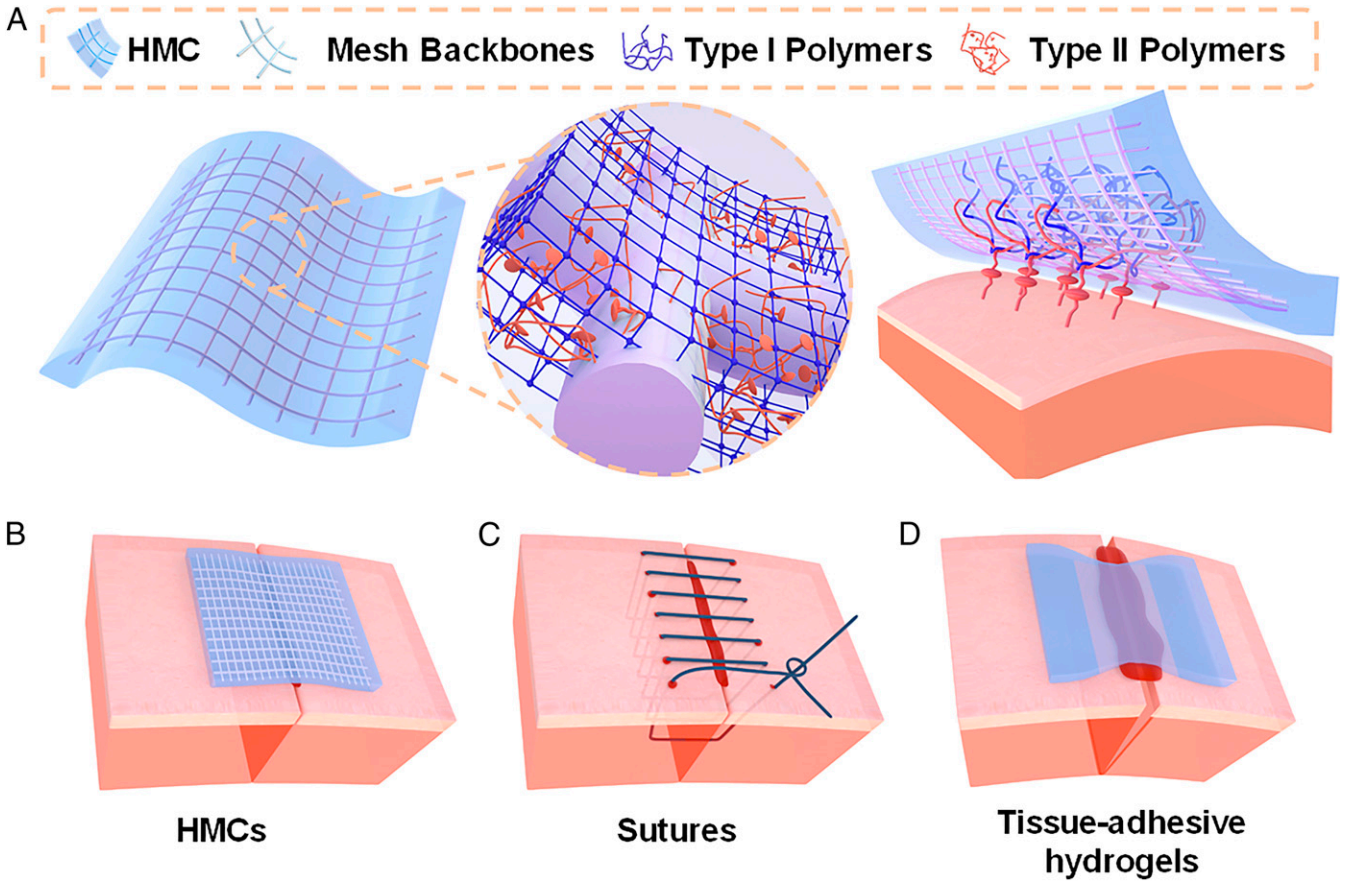

Fig. 1. Design and potential advantage of a hydrogel–mesh composite (HMC). (*A*) Schematic of the HMC. In the HMC, the hydrogel and the surgical mesh form topological entanglement. The hydrogel has long polymer chains of two types: Type I polymers form a covalent network, and type II polymers carry functional groups for adhesion to a tissue. When an HMC contacts a tissue, the hydrogel and tissue adhere through complementary functional groups. Wound closure using three materials: (*B*) HMC, (*C*) suture, and (*D*) tissue-adhesive hydrogel.

By contrast, wound closure by suture causes stress concentration in the tissue (Fig. 1*C*). Also note that a hydrogel by itself is often too weak to resist large tension (Fig. 1*D*). Furthermore, the microscopic pores in the hydrogel, along with the macroscopic pores in the surgical mesh, enable water and other small molecules to migrate in the HMC, so that the HMC can be used as a scaffold for tissue regeneration, as well as a carrier for drug delivery. The HMCs will broaden the applications of surgical mesh in tissue repair, seal, hemostasis, and wound closure, especially on tissues under high mechanical stress.

Results and Discussion

We fabricate an HMC using a particular material system. A surgical mesh woven by polyethylene terephthalate (PET) filaments, with a pore size of ∼50 μm, is placed in a glass mold. Chitosan polymer chains are mixed in the precursor of poly(-*N*-isopropylacrylamide) (PNIPAAm) hydrogel. When the precursor is poured into the mold, the solution infiltrates into the pores of the surgical mesh. In response to ultraviolet (UV) light, the NIPAAm monomers polymerize into a network (Fig. 2*A*). The PNIPAAm network forms intermolecular physical entanglement with the chitosan chains and forms macroscopic topological entanglement with the PET filaments. The HMC integrates chitosan chains, PNIPAAm network, and the PET mesh. The composite is expected to have good biocompatibility. The chitosan chains and the PNIPAAm network have been used in cell culture, drug delivery, and wound dressing (26–29); and the PET mesh has been used as stent graft (30).

We adhere the HMC to a tissue using an aqueous solution of *N*-(3-dimethylaminopropyl)-*N*′-ethylcarbodiimide hydrochloride (EDC)/*N*-hydroxysulfosuccinimide (NHS) coupling agents. The amino groups ($-NH_2$) pendant on chitosan chains form covalent bonds with the carboxyl groups (–COOH) on the tissue (Fig. 2*B*). The PNIPAAm network is hydrophilic below 32 °C, and hydrophobic above (31, 32). In contact with the tissue at the body temperature, the PNIPAAm network shrinks and resists swell (Fig. 2*C*) (33, 34).

A wound closure patch should have large bending compliance to conform to the curved surface of an organ, and large stretch stiffness to resist tissue tension. A hydrogel by itself is easy to bend and easy to stretch. By contrast, the HMC has both large bending compliance and stretch stiffness (Fig. 2*D* and *SI Appendix*, Fig. S2).

We measure adhesion energy between the HMC and various porcine tissues. We spread an aqueous solution of the coupling agent (EDC [1 mmol]/NHS [3 mmol]) onto the surface of a tissue, immediately place an HMC on top, and press for a certain time. The HMC can adhere to a wide variety of tissues, including porcine liver, heart, kidney, skin, and intestine (Fig. 2*E*). The adhesion energies between the HMC and various tissues are 60–120 $J{\cdot}m^{-2}$, which are much higher than those achieved by commercial tissue adhesives (1–10 $J{\cdot}m^{-2}$) (22). The adhesion energy between the HMC and porcine liver increases over time: It reaches ∼70 $J{\cdot}m^{-2}$ within 5 min and attains the maximum of ∼120 $J{\cdot}m^{-2}$ after 1 h (Fig. 2*F*). In surgery, the adhesion with tissues is often desired to be strong and stable during the regeneration

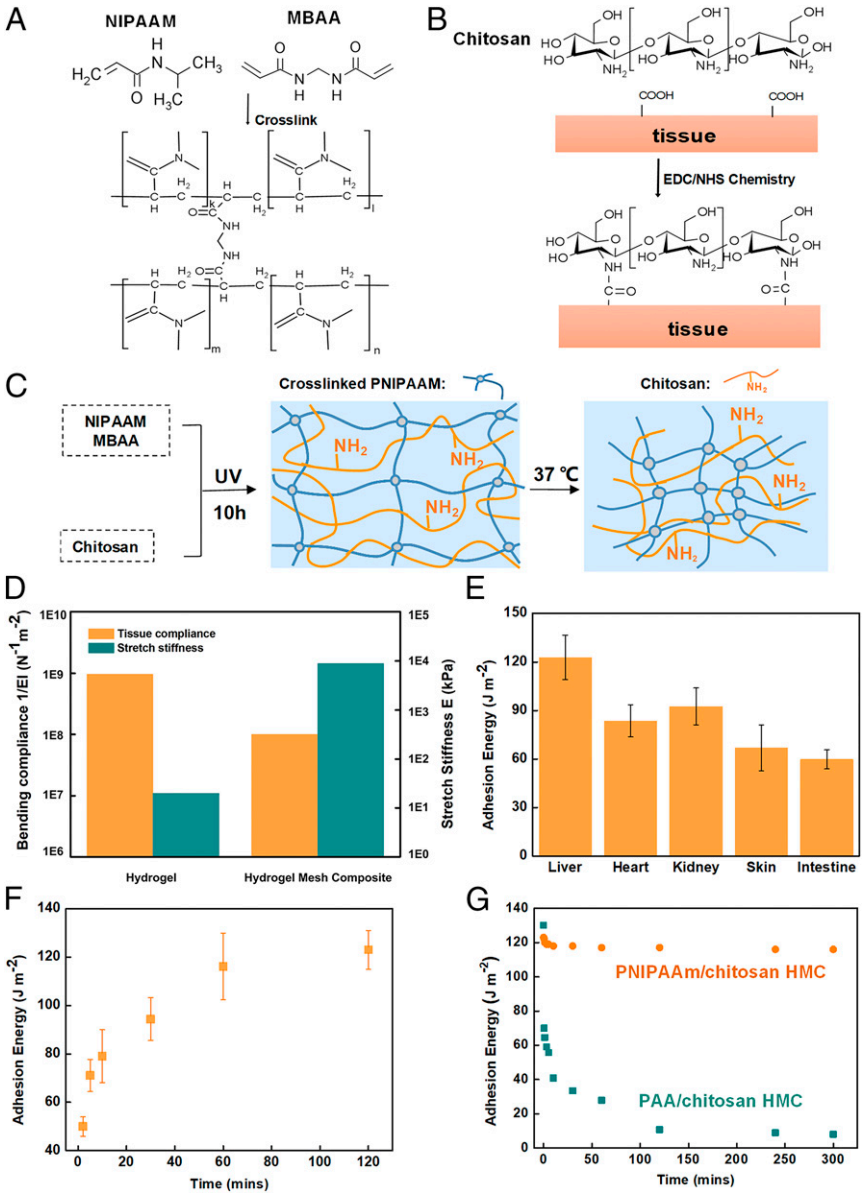

Fig. 2. A hydrogel–mesh composite (HMC), where the hydrogel has long polymers of two types: PNIPAAm (type I) and chitosan (type II). (*A*) PNIPAAm forms a network in topological entanglement with the fibers of the surgical mesh. (*B*) The amino groups on chitosan and carboxyl groups on tissues form covalent bonds, in the presence of EDC and NHS as coupling agents. (*C*) The PNIPAAm network and chitosan chains couple through noncovalent interactions and physical entanglement. Above the phase transition temperature, the PNIPAAm network becomes hydrophobic and resists swell. (*D*) Comparison of the bending and in-plane stretching properties of a hydrogel and an HMC. (*E*) The adhesion between the HMC and various porcine tissues. (*F*) The adhesion energy increases as a function of time. (*G*) At 37 °C, submerged in the PBS solution, a PNIPAAm/chitosan HMC keeps adhesion energy nearly a constant over time, but a PAA/chitosan HMC decreases adhesion energy over time.

of tissues, which may range from several days to weeks (23), as premature failure of the adhesion may cause serious complications such as bleeding and fluid leakage (23). To study the stability of adhesion between the HMC and tissue in the physiological environment, we immersed the adhered HMC and porcine liver in 37 °C PBS solution and monitored the change of adhesion energy over time. Benefitting from the temperature-induced volume phase transition of PNIPAAm network, the adhesion energy remains a constant of ~120 $J{\cdot}m^{-2}$ over 300 min. As a comparison, the adhesion energy of a composite of a swellable poly(acrylic acid) (PAA) hydrogel and PET mesh decreased from the initial value of ~130 to ~30 $J{\cdot}m^{-2}$ in 60 min, and to less than ~10 $J{\cdot}m^{-2}$ after 300 min (Fig. 2*G*). We choose PAA hydrogel for comparison because PAA and PNIPAAm can be synthesized using the same procedure, but they swell differently. The thermo-responsive PNIPAAm network enables a swell-resistant HMC in physiological environment.

The combination of large bending compliance, large stretch stiffness, as well as strong and stable adhesion enables the HMC to be used in surgery. We conduct in vitro experiments using porcine liver. We mount a piece of porcine liver with a 2-cm-diameter hole to a chamber and adhere an HMC with a thickness of 500 μm on the liver to cover the hole (Fig. 3*A*). As a syringe pumps liquid into the chamber, the HMC bulges (Fig. 3*B*). The PET mesh in the HMC works as a skeleton and spreads stress over a large area of the tissue. The adhesion area bulges slightly as a whole when the pressure increases to 185 mm Hg, which is higher than the normal systolic blood pressure (120 mm Hg) in humans. By contrast,

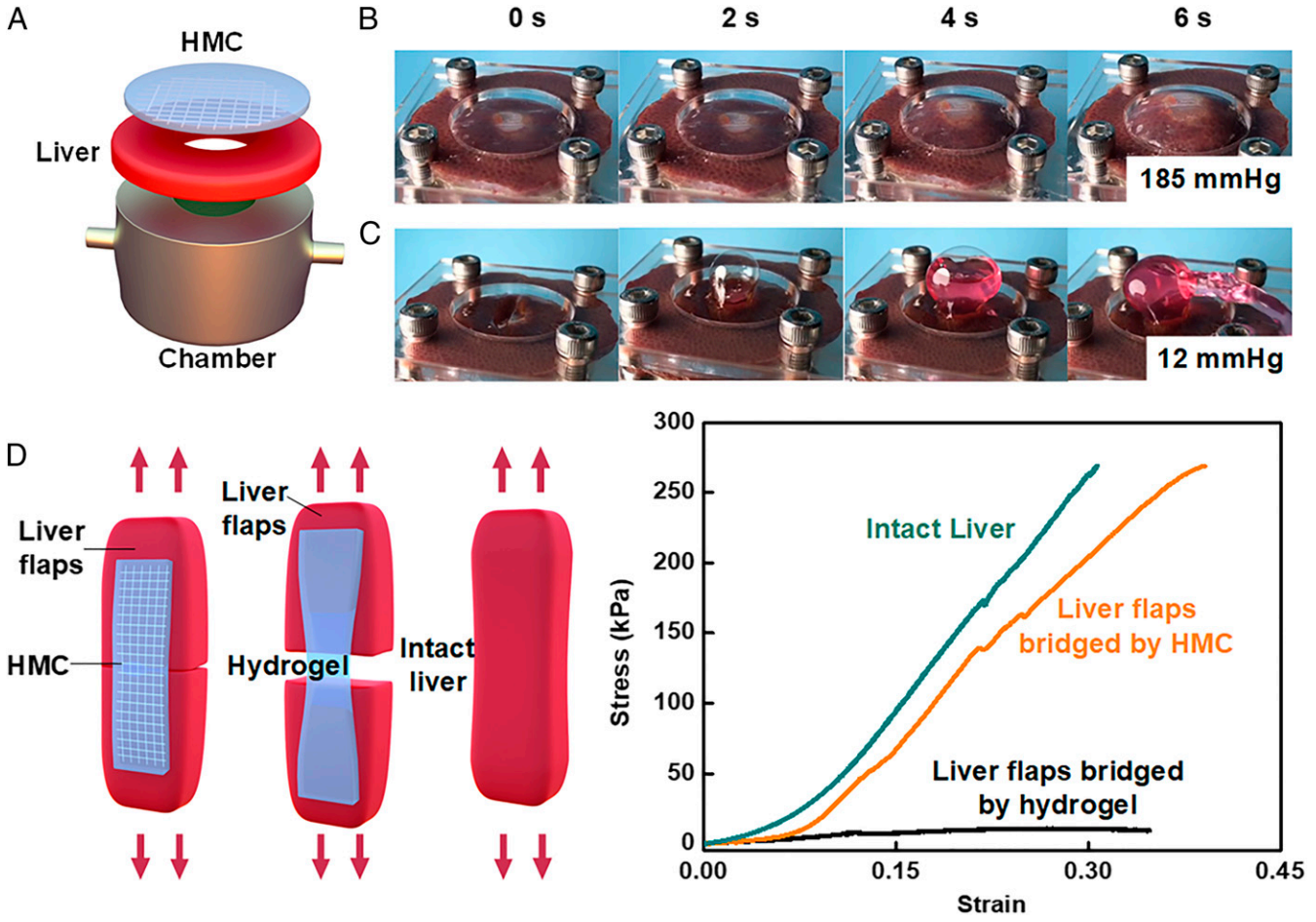

Fig. 3. Mechanical tests of the HMC adhered to wounded tissue. (*A*) Experiment setup to measure burst pressure. Photos of (*B*) the HMC and (*C*) the pure hydrogel adhered on a tissue with a hole and subject to pressure. (*D*) Schematic of the experiment and the measured stress–strain curves of the HMC and pure hydrogel adhered on a tissue with a cut.

when we cover the hole by adhering a PNIPAAm/chitosan hydrogel of the same thickness (500 μm) without the mesh, the burst pressure is 12 mm Hg. The hydrogel ruptures, but adhesion is intact (Fig. 3*C*). For the hydrogel to sustain a pressure above 120 mm Hg, the thickness of the hydrogel must be much thicker, which will be unsuitable for in vivo applications where the space among tissues is limited. We next cut a piece of porcine liver in the middle and bridge the two flaps by adhering an HMC with a thickness of 500 μm on their surfaces. When we stretch the adhered sample on a tensile machine, the tissue flaps maintained close contact until the adhering interface fails. Comparing with an intact liver piece, the adhered sample has a similar tensile strength of ∼270 kPa. However, when the two liver flaps are bridged by a piece of pure hydrogel of the same thickness (500 μm), the sample factures at a stress of ∼20 kPa (Fig. 3*D*).

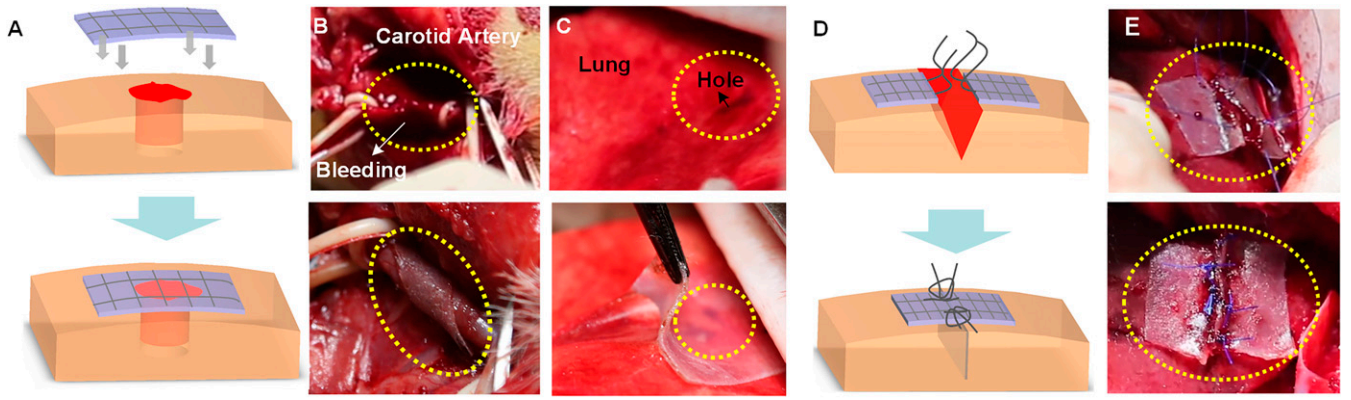

Fig. 4. Applications of the HMC in surgeries of a sheep. (*A*) Schematic of the adhesion of an HMC on a wounded tissue for hemostasis or repair. (*B*) Using the HMC for hemostasis on carotid artery. (*C*) Using the HMC to repair a hole in a lung. (*D*) Schematic of the shoelace-adhesive wound closure by using HMC and sutures. (*E*) Using the shoelace-adhesive wound closure for laceration on liver.

We have tried to sterilize the HMCs using several methods. The HMCs sterilized using common methods, such as autoclaving and Co_{60} radiation, show much reduced adhesion energy in ex vivo adhesion test (*SI Appendix*, Fig. S3). We then sterilize the HMCs as follows. The precursor of the PNIPAAm/chitosan hydrogel is filtered using 0.2-μm sterile syringe filters, and the PET mesh is autoclaved. Then the HMC is cured in a sterile environment. The adhesion energy between such an HMC and tissues decreases only ∼10%.

We evaluate the performances of the HMC in surgeries of a sheep through an acute experiment. An adult sheep (with weight of ∼30 kg) is used as its sizes of organs and amount of bleeding are comparable to a human. We choose three representative tissues for research: the carotid artery, which has high local pressure with rapid and a large amount of blood spurts; the lung, which has less hemorrhage but with relatively high local pressure; and the liver, which has low local pressure but with a large amount of diffuse hemorrhage. We evaluate the hemostasis and immediate sealing effect of the HMC on the three tissue traumas. The HMC can adhere to wounded tissues for hemostasis or repair (Fig. 4*A*). We expose the carotid artery of the sheep and pierce a hole with a needle of 3-mm inner diameter. Bloodstream spurts out immediately due to the high blood pressure. We clamp the blood vessels to stop the blood flow, press an HMC onto the wound for several minutes, and then remove the clamps. The HMC conforms to the curved surface of the artery and forms a strong adhesion with the tissue to stop bleeding (Fig. 4*B* and Movie S1). We further expose the lung of the sheep and make a laceration with a length of ∼2 cm. The defect is repaired by adhering an HMC to prevent the air leakage. The HMC and the lung adhere strongly and are difficult to separate by tweezers (Fig. 4*C* and Movie S2). Different types of tissues have different wall thicknesses. Some tissues are relatively thin. For example, the mean common carotid arterial thickness is ∼0.6 mm (35), and the mean wall thickness of the small bowel is ∼2 mm (36). Sutures or staples for these tissues may cause complications like laceration, anastomotic fistula, errhysis, and infection (37, 38). In these cases, HMCs are expected to have advantages.

We now demonstrate a procedure called the shoelace-adhesive wound closure. We stitch several sutures in two pieces of HMC, adhere the sutured HMCs to a wound, and pull the sutures like shoelaces (Fig. 4*D*). As a demonstration, we made a cut with a length of ∼30 mm on the liver of the sheep and adhere the sutured HMCs along both sides of the incision. Before we pull the sutures, the wound bleeds. After we tighten and knot the sutures, the wound stops bleeding (Fig. 4*E* and Movie S3). In a conventional use of suture, threads are sewn into tissues and pulled to close a wound. The threads concentrate stress and may cause damage. Furthermore, diseased tissues can be too fragile or too stiff to be sutured. By contrast, in a shoelace-adhesive procedure, threads are sewed into HMCs, not into tissues, and the HMCs are adhered to large areas of the tissues. The tension in the threads transfers to the shear in the tissues over a long distance, through the action of shear lag (*SI Appendix*, Fig. S4) (39). The shoelace-adhesive procedure may provide a solution when the tissues are too weak to sew or pull.

Conclusion

In summary, we propose a design called HMC, which broadens the function of surgical mesh by adding one important property: strong adhesion with tissue. The HMC can be fabricated through a wide variety of adhesion strategy and a wide choice of hydrogel material and surgical mesh. Here, we illustrate the concept by using a particular system of PNIPAAm/chitosan HMC, which can form strong and swell-resistant adhesion with various tissues under physiological environment. We demonstrate that the combination of strong adhesion and large stretch stiffness enables the HMC to seal a wound against blood pressure and bridge a cut under tissue tension. We also propose a shoelace-adhesive procedure for wound closure using the HMC. HMCs may open doors to innovation in clinical surgery.

Materials and Methods

Materials. All chemicals were purchased and used without further purification. Monomers including *N*-isopropylacrylamide (NIPAAm) (TCI; I0401) and acrylic acid (AA) (Sigma-Aldrich; 147230), cross-linker *N*,*N*′-methylenebisacrylamide (MBAA) (Sigma-Aldrich; M7279), initiator α-ketoglutaric acid (OA) (Aladdin; K105571) and accelerator *N*,*N*,*N*′,*N*′-tetramethylethylenediamine (TEMED) (Sigma-Aldrich, T7024) were used to synthesize the covalently cross-linked polymer network. Chitosan (medium molecular weight; Sigma-Aldrich; 448877) was used as the long-chain polymer with functional groups for covalent bonding with tissues. Hydrochloric acid solution (HCl) (AR; 10 wt%, Kunshan Jincheng Reagent Company) and sodium hydroxide (NaOH) (AR; Tianjin Zhiyuan Chemical Reagent Company) were used to adjust the pH. EDC (Aladdin; E106172) and NHS (Aladdin; H109330) were used as the coupling agents. The porcine skin, liver, kidney, intestine, and heart for in vitro test were purchased from a local grocery store.

Preparation of PNIPAAm/Chitosan Hydrogel. The synthesis procedure of the hydrogel is similar as described in our previous work (40). NIPAAM (11.22 g) and chitosan (2 g) were first added in deionized water (100 mL), and the pH was adjusted to 5 by dripping HCl solution with a pH meter (Mettler Toledo SevenEasy Series Meters). MBAA (MBAA to NIPAAM weight ratio is 0.0011:1), OA (OA to NIPAAM weight ratio is 0.0013:1), and TEMED (TEMED to NIPAAM weight ratio is 0.0022:1) were then added sequentially. The precursor solution was poured into a reaction vessel, which was made of two parallel glass sheets separated by a 2.0-mm-thick silicone spacer. Then the vessel was exposed to UV light with a wavelength of 365 nm for 10 h.

Preparation of PAA Hydrogel. AA (8.22 g) was dissolved in deionized water (21.78 mL), with the pH adjusted to 7 by concentrated NaOH. MBAA (MBAA to AA weight ratio is 0.0058:1), OA (OA to AA weight ratio is 0.0011:1), and TEMED (TEMED to AA weight ratio is 0.0022:1) were then added sequentially. The precursor solution was poured into a reaction vessel, which was made of two parallel glass sheets separated by a 2.0-mm-thick silicone spacer. Then the vessel was exposed to UV light with a wavelength of 365 nm for 10 h.

Adhesion Procedures. Before treatment, the isolated porcine skin, liver, kidney, intestine, and heart were washed by deionized water. All the isolated tissues, hydrogels, and HMCs were cut into the size of 70 × 15 × 2 mm. In a typical procedure, 200 μL of aqueous solution of EDC (10 wt%) and NHS (10 wt%) were spread on the tissue surface, with a piece of hydrogel (or HMC) pressed on top. The hydrogel (or HMC) and the tissue were pressed together with a strain of 10% for 1 h to achieve adhesion, unless otherwise stated.

Stretch Stiffness and Bending Compliance of the HMC. To measure the stretch stiffness, the specimens (HMC and hydrogel) were cut into dumbbell shape (2 × 12 mm, 35 mm in total length) and fixed to the grippers of a tensile machine (Shimadzu; AGS-X) with a 100-N load cell. The specimens were continuously stretched at a rate of 30 mm·min^{-1} until fracture. The stretch stiffness E was calculated as the slope of the approximately linear part of the stress–strain curve (strain within 10%). The bending compliance was calculated as $1/EI$ (see *SI Appendix, Supplementary text* and Fig. S2 for the details of calculation). All the measurements were repeated three times.

Peeling Tests for Measuring the Adhesion Energy. The measurement of the adhesion energy is similar as described in our previous work (40). A 180° peeling test was used to measure the adhesion energy. All the samples were cut into the same size (70 × 15 × 2 mm). The back sides of all the adherends were glued with 100-μm-thick stiff polyester films by Krazy glue. The free ends of the samples were fixed to the grippers of a tensile machine with 100-N load cells, with a peeling rate of 24 mm·min^{-1}.

Burst Pressure Test. A piece of porcine liver (50 mm in diameter, 3 mm in thickness) with a hole (20 mm in diameter) in the center was first cleaned by deionized water and then fixed to the chamber, which connected with syringe pump filled with PBS solution and a digital manometer to measure the burst pressure. Then, 200 μL of aqueous solution of EDC (10 wt%) and NHS (10 wt%) were spread on the liver surface and a piece of HMC or hydrogel (30 × 30 × 0.5 mm) was pressed on top of the adherent surface for 20 min. The PBS solution was pumped at a constant speed with the syringe pump

and the highest reading on the digital manometer before pressure loss was considered as the burst pressure. All the measurements were repeated three times.

Stress–Strain Curves of Tissue Flaps Bridged by the HMC. A piece of intact liver ($80 \times 15 \times 2$ mm) was cut into two pieces in the middle, and then the two flaps were bridged by adhering a piece of HMC or pure hydrogel ($40 \times 15 \times 0.5$ mm) on tissue surfaces. The specimen was fixed to the grippers of a tensile machine (Shimadzu; AGS-X) with 100-N load cells, and continuously stretched at a rate of 30 mm·min^{-1} until fractures occurred. All the measurements were repeated three times.

In Vivo Tests. All in vivo experiments were reviewed and approved by Xijing Hospital Committee on Animal Care. A female small-tailed Han sheep (with weight of ~30 kg) was used in the experiment. Before the experiment, the sheep was anesthetized at a sterile operating table. The carotid artery of the sheep was first exposed to the air and hemostatic forceps were set on the two ends of the blood vessel to control the blood flow. A 3-mm inner diameter needle was used to pierce the artery vessel. Then the wound surface was quickly cleaned with cotton gauze, and 100 μL of aqueous solution of EDC (10 wt%) and NHS (10 wt%) were spread on the wound surface followed by pressing of the HMC ($4 \times 10 \times 0.5$ mm) on top to cover the wound. The lung of the sheep was exposed to the air and a laceration (20 mm in length) was made on the lung lobe with an operating scalpel. The wound surface was cleaned up with cotton gauze. Two hundred microliters of aqueous solution of EDC (10 wt %) and NHS (10 wt%) were spread on the wound surface followed by pressing of the HMC ($35 \times 35 \times 0.5$ mm) on top to cover the wound.

Shoelace-Adhesive Procedure. Before the experiment, two pieces of HMC ($30 \times 15 \times 0.5$ mm) were placed side by side with their edge threaded by two medical sutures. Then the liver of the sheep was exposed to the air and cleaned up with saline solution and cotton gauze. A laceration (30 mm in length) was made on the liver lobe with an operating scalpel. Two hundred microliters of aqueous solution of EDC (10 wt%) and NHS (10 wt%) were spread on the wound area, and the suture-dressed HMCs were pressed on both sides of the laceration. By tightening and knotting the sutures, the wound can be closed to stop bleeding.

Data Availability. All study data are included in the article and/or supporting information.

ACKNOWLEDGMENTS. This work was supported by the National Natural Science Foundation of China (Grants 11702212, 11922210, and 11772249).

1. M. J. Funk *et al*., Trends in use of surgical mesh for pelvic organ prolapse. *Am. J. Obstet. Gynecol.* **208**, 79e1–79e7 (2013).
2. A. Rastegarpour *et al*., Surgical mesh for ventral incisional hernia repairs: Understanding mesh design. *Plast. Surg. (Oakv.)* **24**, 41–50 (2016).
3. A. Choksey, D. Soonawalla, J. Murray, Repair of neglected Achilles tendon ruptures with Marlex mesh. *Injury* **27**, 215–217 (1996).
4. J. A. Santibáñez-Salgado *et al*., Lyophilized glutaraldehyde-preserved bovine pericardium for experimental atrial septal defect closure. *Eur. Cell. Mater.* **19**, 158–165 (2010).
5. P. K. Narotam, K. Reddy, D. Fewer, F. Qiao, N. Nathoo, Collagen matrix duraplasty for cranial and spinal surgery: A clinical and imaging study. *J. Neurosurg.* **106**, 45–51 (2007).
6. R. W. Luijendijk *et al*., A comparison of suture repair with mesh repair for incisional hernia. *N. Engl. J. Med.* **343**, 392–398 (2000).
7. F. San-Galli *et al*., Experimental evaluation of a collagen-coated vicryl mesh as a dural substitute. *Neurosurgery* **30**, 396–401 (1992).
8. E. Wassenaar, E. Schoenmaeckers, J. Raymakers, J. van der Palen, S. Rakic, Mesh-fixation method and pain and quality of life after laparoscopic ventral or incisional hernia repair: A randomized trial of three fixation techniques. *Surg. Endosc.* **24**, 1296–1302 (2010).
9. E. B. Wassenaar, J. T. F. J. Raymakers, S. Rakic, Impact of the mesh fixation technique on operation time in laparoscopic repair of ventral hernias. *Hernia* **12**, 23–25 (2008).
10. R. K. Kitamura, J. Choi, E. Lynn, C. M. Divino, Suture versus tack fixation of mesh in laparoscopic umbilical hernia repair. *JSLS* **17**, 560–564 (2013).
11. P. Negro *et al*., Open tension-free Lichtenstein repair of inguinal hernia: Use of fibrin glue versus sutures for mesh fixation. *Hernia* **15**, 7–14 (2011).
12. T. Sugawara *et al*., Novel dural closure technique using polyglactin acid sheet prevents cerebrospinal fluid leakage after spinal surgery. *Neurosurgery* **57** (4 suppl.), 290–294, discussion 290–294 (2005).
13. N. Ladwa, M. S. Sajid, P. Sains, M. K. Baig, Suture mesh fixation versus glue mesh fixation in open inguinal hernia repair: A systematic review and meta-analysis. *Int. J. Surg.* **11**, 128–135 (2013).
14. H. Nomori *et al*., Triple-layer sealing with absorptive mesh and fibrin glue is effective in preventing air leakage after segmentectomy: Results from experiments and clinical study. *Eur. J. Cardiothorac. Surg.* **45**, 910–913 (2014).
15. T. Tanaka, K. Ueda, J. Murakami, K. Hamano, Use of stitching and bioabsorbable mesh and glue to combat prolonged air leaks. *Ann. Thorac. Surg.* **106**, e215–e218 (2018).
16. H. Kunou *et al*., Two cases of air leak syndrome after bone marrow transplantation successfully treated by the pleural covering technique. *Gen. Thorac. Cardiovasc. Surg.* **67**, 987–990 (2019).
17. Y. Shimada *et al*., Dural substitute with polyglycolic acid mesh and fibrin glue for dural repair: Technical note and preliminary results. *J. Orthop. Sci.* **11**, 454–458 (2006).
18. S. Masuda *et al*., The dural repair using the combination of polyglycolic acid mesh and fibrin glue and postoperative management in spine surgery. *J. Orthop. Sci.* **21**, 586–590 (2016).
19. A. Hayashibe, K. Sakamoto, M. Shinbo, S. Makimoto, T. Nakamoto, New method for prevention of bile leakage after hepatic resection. *J. Surg. Oncol.* **94**, 57–60 (2006).
20. S. Kobayashi *et al*., Fibrin sealant with polyglycolic acid felt vs fibrinogen-based collagen fleece at the liver cut surface for prevention of postoperative bile leakage and hemorrhage: A prospective, randomized, controlled study. *J. Am. Coll. Surg.* **222**, 59–64 (2016).
21. J. Li *et al*., Tough adhesives for diverse wet surfaces. *Science* **357**, 378–381 (2017).
22. H. Yuk *et al*., Dry double-sided tape for adhesion of wet tissues and devices. *Nature* **575**, 169–174 (2019).
23. G. M. Taboada *et al*., Overcoming the translational barriers of tissue adhesives. *Nat. Rev. Mater.* **5**, 310–329 (2020).
24. B. R. M. Perrin *et al*., Adhesion of surgical sealants used in cardiothoracic and vascular surgery. *Int. J. Adhes. Adhes.* **70**, 81–89 (2016).
25. N. Gillman, D. Lloyd, R. Bindra, R. Ruan, M. Zheng, Surgical applications of intracorporal tissue adhesive agents: Current evidence and future development. *Expert Rev. Med. Devices* **17**, 443–460 (2020).
26. L. Klouda, Thermoresponsive hydrogels in biomedical applications: A seven-year update. *Eur. J. Pharm. Biopharm.* **97** (Pt B), 338–349 (2015).
27. S. O. Blacklow *et al*., Bioinspired mechanically active adhesive dressings to accelerate wound closure. *Sci. Adv.* **5**, eaaw3963 (2019).
28. V. Bhagat, M. L. Becker, Degradable adhesives for surgery and tissue engineering. *Biomacromolecules* **18**, 3009–3039 (2017).
29. H. Kamata, Y. Akagi, Y. Kayasuga-Kariya, U. I. Chung, T. Sakai, "Nonswellable" hydrogel without mechanical hysteresis. *Science* **343**, 873–875 (2014).
30. G. W. Stone *et al*., Prospective, randomized, multicenter evaluation of a polyethylene terephthalate micronet mesh-covered stent (MGuard) in ST-segment elevation myocardial infarction: The MASTER trial. *J. Am. Coll. Cardiol.* **60**, 1975–1984 (2012).
31. Y. Hirokawa, T. Tanaka, Volume phase-transition in a nonionic gel. *J. Chem. Phys.* **81**, 6379–6380 (1984).
32. O. Erol, A. Pantula, W. Q. Liu, D. H. Gracias, Transformer hydrogels: A review. *Adv. Mater. Technol.* **4**, 1900043 (2019).
33. B. L. Ekerdt *et al*., Thermoreversible hyaluronic acid-PNIPAAm hydrogel systems for 3D stem cell culture. *Adv. Healthc. Mater.* **7**, e1800225 (2018).
34. C. Cheng, D. D. Xia, X. L. Zhang, L. Chen, Q. Q. Zhang, Biocompatible poly(*N*-isopropylacrylamide)-g-carboxymethyl chitosan hydrogels as carriers for sustained release of cisplatin. *J. Mater. Sci.* **50**, 4914–4925 (2015).
35. J. F. Polak *et al*., Carotid-wall intima-media thickness and cardiovascular events. *N. Engl. J. Med.* **365**, 213–221 (2011).
36. A. C. Fleischer, C. A. Muhletaler, A. E. James Jr, Sonographic assessment of the bowel wall. *AJR Am. J. Roentgenol.* **136**, 887–891 (1981).
37. A. P. Duarte, J. F. Coelho, J. C. Bordado, M. T. Cidade, M. H. Gil, Surgical adhesives: Systematic review of the main types and development forecast. *Prog. Polym. Sci.* **37**, 1031–1050 (2012).
38. N. Annabi *et al*., Surgical materials: Current challenges and nano-enabled solutions. *Nano Today* **9**, 574–589 (2014).
39. H. L. Cox, The elasticity and strength of paper and other fibrous materials. *Br. J. Appl. Phys.* **3**, 72–79 (1952).
40. Y. Gao *et al*., A universal strategy for tough adhesion of wet soft material. *Adv. Funct. Mater.* **30**, 2003207 (2020).